Synthesis, Characterisation and Biological Activity of Polymeric Metal Complexes Derived from Multidentate Ligand

Raghad Usama Abass[1], Enaam Ismail Yousif[2]*

[1, 2]Department of Chemistry, College of Education for Pure Science (Ibn Al-Haitham), University of Baghdad, Adhamiyah, Baghdad, Iraq.

Email: enaamismail@yahoo.com; anaam.i.y@ihcoedu.uobaghdad.edu.iq

Abstract

New Schiff-base ligand and their polymeric metal complexes with Cr(Ш), Mn(II), Fe(II),Co(II),Ni(II) and Cu(II) ions are reported. Ligand was prepared in two-step reaction. The reaction of 2-hydroxy-5-methylisophthalaldehyde with 3-Amino-1-propanol resulted in the isolation of precursor (3,3'-((1E,1'E)-(propane-1,3-diylbis (azanylylidene)) bis (methanylylidene)) bis (2-hydroxy-5-methylbenzaldehyde)).The reaction of precursor with acrylamide gave the required ligand; (N,N'-((1E,1'E)-(((1E,1'E)-(propane-1,3-diylbis (azanylylidene)) bis (methanylylidene)) bis (2-hydroxy-5-methyl-3,1-phenylene)) bis (methanylylidene)) diacrylamide) H2L. The reaction of this ligand with the appropriate metal ions gave polymeric metal complexes of the formulae {[M2(L)Cl2]. Cl2H2O} n M=Cr(Ш), {[M2(L) (H2O)2]. Cl2} n M=Mn (II) Ni (II), {[M2(L) (H2O) Cl] Cl} nM=Fe (II), {[M2(L)Cl2]. H2O} n, M= Co (II), Cu (II). A range of techniques was used to confirm the entity of ligand and their complexes. The formation of ligand and mode of complexation and geometrical structure of the title polymeric complexes were verified using FTIR, electronic spectra, NMR, ESMS, magnetic susceptibility, micro-elemental analysis, metal content, chloride content and conductance. The analytical and spectroscopic data indicated the formation of six-coordinate complexes. Biological evaluation of ligand and their polymeric complexes against gram-positive bacteria (G+), Bacillus stubtili, Staphylococcus aureus, and gram-negative bacteria (G−), Escherichia coli and Pseudomonas aeruginosa and compared with antibiotic drug (Cefotaxime) and two types of fungi namely (Candida albicans and Rhizopus sporium) and compared with the activity of fungal agent (Fluconazole).The collected data revealed the antimicrobial activity of the ligand was enhanced upon complex formation.

Keywords: Schiff-base ligand, Acrylamide, Polymeric complexes, Structural study, biological evaluation.

1. Introduction

Polymeric complexes are of current interest due to their potential applications in supramolecular and environmental chemistry and medicine [1, 2]. One approach in the field of supramolecular chemistry has been to investigate the use of polymeric ligands to develop complexes with metal centres that have unusual coordination and new properties. Metal polymeric complexes also have applications in inhibition of tumour growth [3] drug delivery [4], and catalysis [5]. An example of this is the formation of Ru, Rh, Pd and Pt, complexes of polymeric 1-acrylamido-2-(2-pyridyl) ethane. It has been demonstrated that the polymeric ligand plays a role in the reduction of Rh (III) to Rh (II) and Ru (III) to Ru (II) [6]. An important new focus for environmental inorganic chemistry has been the selective removal of metal ions from aqueous solution, including waste treatment, with polymer supported chelate systems. These systems can be prepared either by polymerisation of chelate monomers or by derivatisation of functionalised polymers [7-11]. Schiff-base compounds have a great importance in coordination chemistry, due to their ability to form a range of complexes which have applications in different fields. One approach in the field of coordination chemistry has been to investigate the use of Schiff-base ligands to develop hydroxo-bridged binuclear complexes with homo metallic and/or hetero metallic centers that have interesting magnetic, catalytic properties, electric or optical [12-14]. In the present work we report the synthesis and characterization of some complexes of a polymer derived from the new (N, N'-((1E,1'E) - (1E,1'E) - (propane-1,3-diylbis (azanylylidene)) bis (methanylylidene)bis(2-hydroxy-5-methyl-3,1-phenylene) bis (methanylylidene) diacrylamide) Schiff base

2. Experimental

3. Materials and Methods

Reagents that purchased from Aldrich were used as received. Solvents were dried using standard protocols prior to their use in the preparation.

Measurement techniques

Melting points were recorded without corrections on an Electro-thermal Meltter Toledo MP90 melting point apparatus. Micro-elemental analyses (C.H.N) were carried out on (Eager 300 for EA1112). The FTIR spectra of compounds were recorded using KBr and CsI discs from 4000–200cm-1 on a Shimadzu Fourier Transform Infrared Spectrometer (FTIR-600). The UV-

doi.org/10.31838/hiv22.02.463 Received: 13.04.22, Revised: 27.05.22, Accepted: 04.08.22

Vis spectra of samples with 10-3 M concentration in DMSO solutions at room temperature were measured from 200-1100 nm using a Shimadzu 1800 spectrophotometer. A positive mode Electrospray (ES) mass spectroscopy was used to measure the mass spectra for ligand. 1H-NMR spectra was recorded in DMSO-d6 solutions on Brucker 400 MHz spectrometer. Tetramethylsilane (TMS) was used as an internal standard for 1H NMR analysis. The percentage of metals and chloride content were acquired using atomic absorption spectrophotometer (on a Shimadzu (A.A) 680 G) and potentiometer titration method (on a 686-Titrp processor-665 Dosim A-Metrohm/Swiss), respectively. Molar conductance was performed on a PW 9526 apparatus with DMSO solutions. The magnetic susceptibility measurements were made at room temperature with a magnetic susceptibility balance (Sherwood Scientific). The chloride content for complexes was determined using the potentiometric titration method on 686–Titro Processor-665 Dosim A-Metrohm/Swiss. Thermogravimetric analysis (TGA) was carried out on STA PT-1000 Linseis Company/Germany. The biological evaluation of the ligand and its metal complexes against four bacterial species (Escherichia coli, Pseudomonas aeruginosa, Staphylococcus aureus and Bacillus stubtilis) and compared with antibiotic drug (Cefotaxime) and two types of fungi (Candida albicans and Rhizopus sporium) and compared with the activity of fungal agent (Fluconazole) were performed using agar-well diffusion approach. In this method, the wells were dug in the media with the help of a sterile metallic borer with centres of at least 6mm. Recommended concentration (100µL) of the test sample of 1mg/mL in DMSO was introduced in the respective wells. The plates were incubated immediately at 37°C for 24h. The activity was evaluated by measuring the diameter of inhibition zones (mm).

Synthesis

Synthesis of precursor

The preparation of precursor (3,3'-((1E,1'E) - (propane-1,3-diylbis (azanylylidene)bis (methanylylidene)) bis (2-hydroxy-5-methylbenzaldehyde)) .

A precursor was prepared according to the literature [14]. 3-Amino-1-propanol was added to a EtOH solution 30ml (0.5g, 1.5mmol) was added to 2-hydroxy-5-methylisophthalaldehyde (0.5g, 3.1mmol) with few drops' bromic acid. The resulting solution was refluxed for 4hr and heated at 80°C. The light-yellow precipitate was isolated by filtration. Purer product was obtained by means of washed from hot ethanol and dried at air. Yield: 0.25g,(43%) and m.p = 150-152°C. Elemental analysis: (C.H.N Found, (Calc. %); C=68.35 (68.84), H= 5.92 (6.05), N=7.12(7.65),FT-IR data cm-1:3414 ν(O-H), 1685ν(C=O),1666,1620 δ(C=N), 1543ν(C=C)aromatic, 1238 ν (C-O), 1095 ν (C-N),3066 (C-H)aromatic, 2981(C-H)aliphatic.

Synthesis of Schiff-base ligand H2L

H2L was prepared according to the literature [11]. A solution of acrylamide (0.16g, 2.3mmol) containing HBr 2drops, 48% in ethanol 10ml was added slowly to a mixture of (3,3'-((1E,1'E) -(propane-1,3-diylbis (azanylylidene)) bis(methanylylidene)) bis (2-hydroxy-5-methyl benzaldehyde) (5g, 13.7mmol) in 20ml ethanol. The reaction mixture was heated at 85°C under reflux for 5hr, off-white solid was formed. The solid was filtered off and washed from hot ethanol, (Fig.1). Yield: 3.2g (50%), m.p = 169-171°C. Elemental analysis: (C.H.N Found, (Calc. %); C=68.11(68.63), H= 5.45 (5.97), N=11.45 (11.86), FT-IR data cm-1 :3410 ν(O-H), 1670ν(C=O), 1627 δ(C=N), 1549ν(C=C)aromatic, 1384 ν (C-O), 1238 ν (C-N),3059 (C-H)aromatic, 2981(C-H)aliphatic.

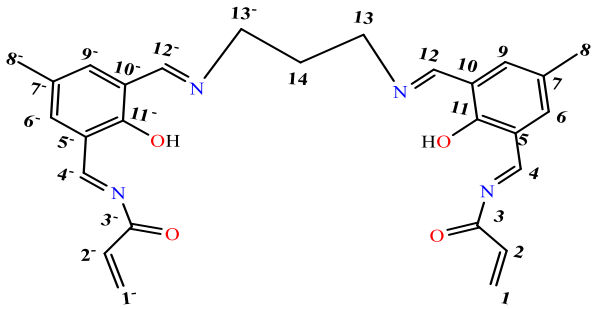

Fig.1: Chemical structure of ligand H_2L.

General synthesis procedure of the polymeric complexes

prepared according to the literature [11]. A mixture of the H2L (1mmol) in ethanol 15ml containing KOH (2mmol) was added over 15min to a stirred solution of metal chloride (2mmol) in hot ethanol 15ml ammonium persulfate (APS) (2mmol) in ethanol 30ml as the initiator. The resulting mixture was refluxed for 4hr at 70-85°C, resulting in the formation of a coloured solution. The solution was concentrated by slow evaporation of the ethanol at RT. The solid mass formed was collected by filtration and washed with EtOH 10ml and finally with diethyl ether 15ml, (Scheme 1). Yields, Colours, Metal salts quantities, melting points for the complexes are listed in (Table 1).

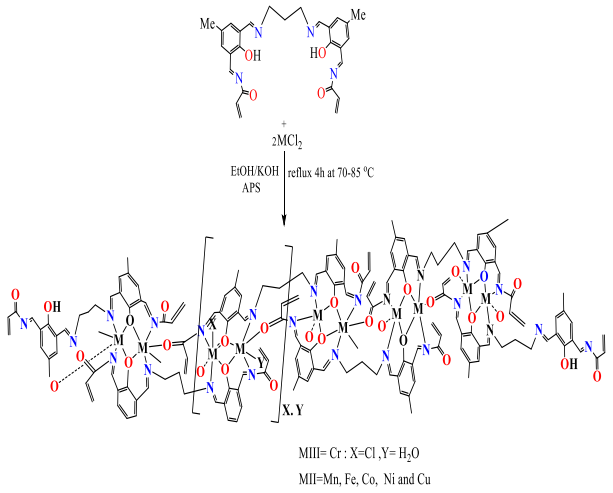

Scheme 1: Synthesis route of H_2L complexes.

Table 1: Yields, Colours, Metal salts quantities, Melting points of complexes.					
Complex	Weight of metal salt (g)	Weight of complex(g)	Yield (%)	Colour	m.p. °C
[Cr2(L)Cl2]. Cl2H2O.	0.13	0.2	51	Yellow	350*
[Mn2(L) (H2O)2]. Cl2.	0.14	0.2	55	Brown	350*
Fe2(L) (H2O) Cl] Cl	0.10	0.15	42	Pale brown	350*
Co2(L)Cl2]. H2O	0.12	0.2	56	Pink	350*
[Ni2(L) (H2O) 2] Cl2	0.14	0.2	54	Greenish - yellow	350*
[Cu2(L)Cl2]. H2O	0.09	0.23	63	Blue green	350*

Microbiological Evaluation

The sensitivity of bacteria and fungi against the prepared compounds were explored by Kirby-Bauer method. In this work, the colony of organism was mixed with a solution of 85% NaCl, until the suspension becomes (0.5 Mcf). This suspension was applied on the surface of a Petri dish filled with Mueller Hinton agar. The holes were made with the same distance and exact concentration. Recommended concentration (100µL) of the test sample 1mg/mL in dimethylsulfoxide was introduced in the wells. The dishes were incubated for 24 h at 37°C and the inhibition zones were measured and compared with standard values [15]. The role of dimethylsulfoxide solutions in the microbiological evaluation were examined separately that indicated no activity against any bacterial strains or fungi species.

4. Results and Discussion

The new Schiff-base ligand is isolated in good yields from the reaction of the acrylamide with (3,3'-((1E, 1'E) - (propane-1,3-diylbis (azanylylidene) bis (methanylylidene) bis(2-hydroxy-5-methylbenzaldehyde). The ligand is prepared in two steps using ethanol as the reaction medium. The H2L is a monobasic ligand that has the ability to form binuclear phenoxo-bridged complexes. The ligand is characterised by CHN, FTIR, UV-Vis and 1H- NMR spectra. The polymeric complexes of Cr(Ш), Mn(II), Fe(II), Co(II), Ni(II) and Cu(II) were synthesised by reacting 1mmole of H2L with 2mmole of the metal chloride, respectively using ethanol as a medium, resulted in the isolation of six r-coordinate monomeric compounds of the general formulae {[M2(L)Cl2].Cl2H2O}n ,M=Cr(Ш),{[M2(L)(H2O)2].Cl2}n, M=Mn(II),Ni(II), {[M2(L)(H2O)Cl]Cl}n, M= Fe(II),{[M2(L)Cl2].H2O}n, M= Co(II),Cu(II), Scheme1. The solid complexes are air-stable and soluble only in DMF and in DMSO with heating, and not soluble in other common organic solvents. The solubility behavior may account for the formation of polymeric species [13]. Eventually, upon complexation, the steric factors that facing the metal centers in the Schiff-base and the involvement of the acrylamide moiety in the coordination will avert the coordination of all binding atoms to a two-metal ion to form binuclear complexes. Further, the required structural influence of H2L assists in the fabrication of chain assemblies of polymeric complexes [15]. Therefore, in this circumstance, the nitrogen atom of the acrylamide segment takes an essential part in the occupation of the empty position on the unsaturated metal center that resulted in the fabrication of ladder-type assemblies. The expected geometries of the complexes were concluded from their spectral and other analytical information. The analytical data (Table 2) supported the proposed formulae. The assignments of the main FT-IR peaks of the ligand and their polymeric complexes are collected in (Table 3). The UV-Vis spectra of the ligand and their polymeric complexes are listed in (Table 4).

Table 2: Micro analysis and physical properties of complexes.							
Complex	Molecular formula	M.Wt	Micro analysis found, (calculated)%				
			C	H	N	M	Cl
[Cr2(L)Cl2]. Cl2H2O.	C27H28Cl4Cr2N4O5	734.68	44.01 (44.14)	3.71 (3.84)	7.50 (7.63)	13.95 (14.13)	19.21 (19.38)
[Mn2(L) (H2O)2]. Cl2.	C27H30Cl2Mn2N4O6	687.01	47.05 (47.20)	4.27 (4.40)	8.00 (8.16)	15.82 (15.99)	10.22 (10.36)
[Fe2(L) (H2O) Cl] Cl	C27H28Cl2Fe2N4O5	671.38	48.21 (48.30)	4.02 (4.20)	8.23 (8.35)	16.47 (16.64)	10.29 (10.61)
[Co2(L)Cl2]..H2O	C27H28Cl2Co2N4O5	677.54	47.69 (47.86)	4.00 (4.17)	8.11 (8.27)	17.27 (17.40)	10.39 (10.50)
[Ni2(L) (H2O) 2] Cl2	C27H30Cl2Ni2N4O6	695.03	46.51 (46.65)	4.21 (4.35)	7.93 (8.06)	16.73 (16.88)	10.11(10.24)
[Cu2(L)Cl2]. H2O	C27H28Cl2Cu2N4O5	686.34	47.13 (47.25)	3.95 (4.11)	8.00 (8.17)	18.27 (18.45)	10.15 (10.37)

FT-IR and NMR Spectra

The FT-IR spectra of the ligand exhibited prominent peaks at 3410,1670,1627,1539,1238 and 1095 due to ν(O-H), ν(C=O), ν(C=N), ν(C=C), ν(C-O) and ν(C-N), respectively [16-19]. After complexation, the FT-IR spectra of the polymeric complexes indicated bands with the appropriate shifts and the M-N and M-O peaks that related to complexation (Table 3). Upon complexation, a band at 1670cm-1 attributed to ν(C=O) of the ligand carbonyl group, which was moved to lower frequencies at 1616-1654. These peaks were shifted to a lower frequency in comparison with that in the ligand indicating the coordination to the metal center. The ν(C=N) of the imine groups is shifted and observed around 1450-1577 cm-1 in complexes indicating the coordination of the imine group to the metal atoms.

These bands were moved to a lower frequency in comparison with that in the ligand. This is due to delocalisation of electron density (t2g) of the metal center to the π-system of the ligand [20-23]. The band appeared at 1539cm-1 can be referred to aromatic(C=C) stretching of the ligand. The ν(C=C) is shifted and observed around 1450-1577 cm-1 in complexes indicating the coordination of the ν(C=C) group to the metal atoms. The band at 1384cm-1 that due to ν(C-O) phenoxo in the ligand is shifted to a lower frequency, upon complexation and appeared about 1319-1377 cm-1 in the phenoxo-bridged complexes. This shift confirms the involvement of the phenoxo-oxygen atom in the coordination to the metal ion in a bridging mode [23]. The band at 1238cm-1 that due to ν(C-N) in the ligand is shifted to a lower frequency, upon complexation and appeared around 1103-1176cm-1 in the ν(C-N) complexes. This is in accordance with previous work reported in the literature [24]. The metal complexes spectrum revealed additional bands between (600-200) cm-1 that were not presented in the H2L spectrum. Bands related to ν(M-O) phenol and ν(M-O) amid were detected range at (682-624) cm - 1 and (590-516) cm-1 [25]. The FT-IR spectra detected peaks correlated to ν(Cr-N), ν(Mn-N), ν(Fe-N), ν(Co-N), ν(Ni-N) and ν(Cu-N),respectively, range at (447-405)cm-1[151-154].The FT-IR spectra revealed bands that belongs to ν(Cr-Cl),ν(Fe-Cl),ν(Co-Cl) and ν(Cu-Cl) at 279;214, 273;227, 275;239 and 287;227cm-1, respectively [25]. In complexes Mn (II), Fe (II) and Ni (II) a band that was detected at 786,759 and 802cm-1 is related to ν(M-OH2). Finally, a band detected at 3483-3329cm−1 was correlated to aqua water molecules. The 1H NMR spectra of H2L is illustrated in (Fig 2). A signal at 8.78ppm that belongs to OH equivalent to two protons (2H, O-H, s). A signal at 8.57ppm that belongs (C4,4,)-H to proton of (2H, s) and a signal at 6.94ppm that belongs (C12,12,)-H to proton of (2H, s). The chemical shift at 6.87ppm that equivalent to two proton and appear as single is related to (C9,9,)-H (2H, s). The chemical shift at 6.75ppm that equivalent to two protons and appears as a singlet is related to(C6,6,)-H (2H, s). The triplet peak at 6.67-6.63ppm that is equal to two protons are allocated to the C1-H (C2,2,)-H ((2H, t, J = 16Hz). The doublet peak at 6.44-6.41ppm that equivalent to protons assigned to the C1-H (C1,1,)-H (4H, d, J = 12Hz). The triplet peak at 4.25-4.22ppm that is equal to protons are allocated to the -N-CH2 (C13,13,)-H (C13,13,)-H (4H, t, J= 12Hz). The multiplet peak at 1.67-1.65ppm that equivalent to protons assigned to the -CH3 (C8,8,)-H (6H, s, -(Me).

Table 3: The FT-IR spectral data of complexes (cm-1).

Complex	ν(C=O)	ν(C=N) ν(C=C) aro	ν(C-O)	ν(C-N)	ν(H2O) ν(M-OH2)	ν(M-O) pho ν(M-O) amid	ν(M-N)	ν(M-Cl)
H_2L	1670	1627 1539	1384	1238	-	-	-	-
$[Cr_2(L)Cl_2].Cl_2H_2O.$	1651	1620 1458	1361	1176	3441	682 578	424	279, 214
$[Mn_2(L)(H_2O)_2].Cl_2.$	1662	1654 1558	1323	1172	3394 786	632 543	455	-
$[Fe_2(L)(H_2O)Cl].Cl$	1662	1620 1577	1319	1103	3329 759	651 588	447	273
$[Co_2(L)Cl_2].H_2O$	1635	1616 1458	1354	1172	3417	624 590	405	275 239
$[Ni_2(L)(H_2O)_2]Cl_2$	1651	1624 1450	1377	1176	3483 802	644 524	424	-
$[Cu_2(L)Cl_2].H_2O$	1654	1624 1454	1354	1172	3394	628 516	412	287 227

Mass spectrum

The mass spectrum of H2L a molecular weight peak at m/z = 472 amu is not shown. The peak recorded in 413.25amu belongs to (C25H23N3O3+4), (Fig 3) related to M-(C25H23N3O3+4). The suggested fragmentation pattern is shown in (Scheme 2). Peaks seen at 413.25(10%), 341.41(7%), 281.34(20%),207.23(25%) and 91.09(33%)amu attributed to[M-(C25H23N3O3+4)], [M-(C25H23N3O3+4)+(C19H23N3O3)], [M-(C25H23N3O3+4) + (C19H23N3O3) +(C17H17N2O2.)], [M-(C25H23N3O3+4)+(C19H23N3O3)+(C17H17N2O2.)+(C14H9NO)] and [M-(C25H23N3O3+4)+(C19H23N3O3)+(C17H17N2O2.)+(C14H9NO)+(C6H3O.)], respectively or [M-(C25H23N3O3+4)], [M-(C25H23N3O3+4)+(C19H23N3O3)], [M-(C25H23N3O3+4)+(C19H23N3O3)+ (C18H26N3O2+3)], [M-(C25H23N3O3+4)+(C19H23N3O3)+(C18H26N3O2+3)+(C8H10+2)] and [M-(C25H23N3O3+4)+(C19H23N3O3) +(C18H26N3O2+3)+(C8H10-2.) +(C6H3O.).

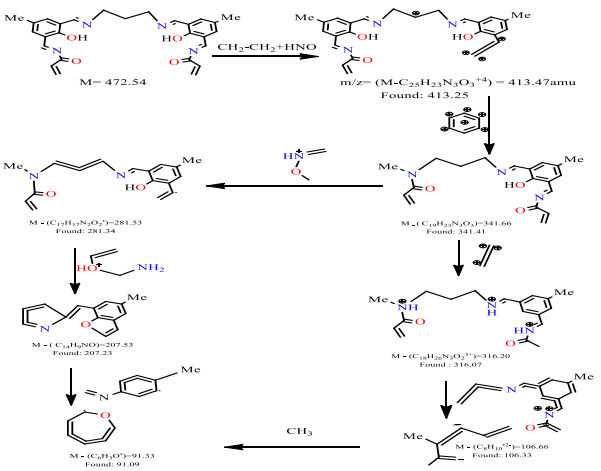

Scheme 2: The fragmentation pattern and relative abundance of H_2L fragments.

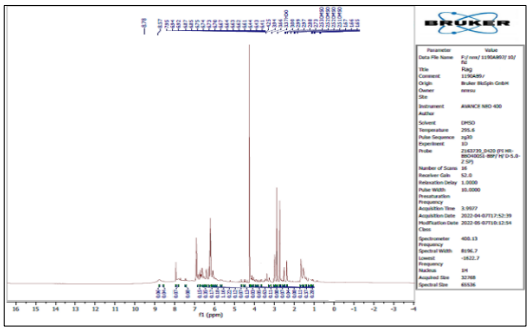

Fig 2: The ^1H -NMR spectrum of H_2L.

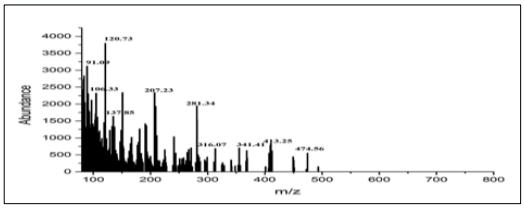

Fig 3: The electrospray (+) mass spectrum of H_2L.

Electronic spectra and magnetic moments measurements

The complexes' electronic spectra, magnetic moments measurements data are collected in (Table 4). Various peaks around 266-280nm are seen in the electronic spectra of the complexes, which are attributable to $\pi \rightarrow \pi*$ and $n \rightarrow \pi*$, respectively. Charge transfer (C.T) is responsible for additional peaks at 300-424nm [26,27]. At 674nm, the electronic spectrum of Cr (III) exhibits band due to 4A2g→4T2g, revealing a deformed octahedral structure around the Cr (III) center. The deformed octahedral shape agrees with the magnetic moment value μeff =3.05BM of Cr (III). The electronic spectra of Mn (II) show a band in the d-d region at 665 and 685nm that are caused by 6A1g →4Eg (4D) and 6A1g →4T1g(4G), revealing a deformed octahedral structure. The measured magnetic moment value μeff =4.16BM is consistent with the Mn (II)-complex, which has a deformed octahedral configuration around the Mn atom. Fe (II) has bands in the d-d region at 874 and 906nm that are visible in its electronic spectrum due to 5T2g →5Eg and 5T2g →5Eg around the Fe (II)center, revealing a deformed octahedral structure. The measured magnetic moment value μeff =3.81BM is consistent with the Fe (II)-complex, which has a deformed octahedral configuration around the Fe atom [27,28]. At 677,775 and 823nm, a band in the Co (II)-complex assigned to 4T1g(F)→4T2g(F), 4T1g(F)→4T2g(F) and4T1g(F)→4T2g(F) were detected, indicating a octahedral configuration around the metal center. The octahedral shape agrees with the magnetic moment value μeff =2.72BM of Co (II). Ni (II) complex spectrum revealed a peak at 412and775nm, which was attributed to 3A2g(F)→3T1g(P) and 3A2g(F)→3T2g(F). Ni-complex with deformed octahedral structure exhibit these transitions [27,29]. the distorted octahedral geometry agrees with the magnetic moment value μeff =1.75BM of Ni (II). The electronic spectra of Cu (II) show a band in the d-d region at 893 nm that are caused by 2Eg→2T2g, revealing a deformed octahedral structure The measured magnetic moment value μeff =1.42BM is consistent with the Cu (II) -complex, which has a deformed octahedral configuration around the Cu atom [27,29].

Table 4:The electronic spectra data of complexes and magnetic moment and conductivity.

Comp.	Band Position λ_{nm}	Wave number (cm^{-1})	Extinction coefficient ε_{max} ($dm^3\ mol^{-1}\ cm^{-1}$)	Assignment	μeff (BM)	Λm S.cm2.mole $^{-1}$	Suggested geometry
[Cr2(L)Cl2]. Cl2H2O.	270 424 674	37037 23584 14836	1787 213 125	Intra-ligand π → π*, n→π* C.T 4A2g→4T1g	3.05	81	Distorted octahedral
[Mn2(L) (H2O)2]. Cl2.	266 425 665 683	37593 23529 15037 14641	1118 491 258 203	Intra-ligand π → π*, n→π* C.T 6A1g →4Eg (4D) 6A1g →4T1g(4G)	4.16	85	Distorted octahedral
Fe2(L) (H2O) Cl] Cl	270 334 874 906	37037 29940 11442 11038	1735 972 33 39	Intra-ligand π → π*, n→π* C.T 5T2g →5Eg 5T2g →5Eg	3.81	40	Distorted octahedral
Co2(L)Cl2].H2O	278 300 677 775 823	35971 33333 14771 12903 12151	359 135 371 46 45	Intra-ligand π → π*, n→π* C.T 4T1g(F)→4T2g(F) 4T1g(F)→4T2g(F) 4T1g(F)→4T2g(F)	2.72	20	Distorted octahedral
[Ni2(L) (H2O) 2] Cl2	280 350 412 775	35714 28571 24271 12903	587 1500 110 52	Intra-ligand π → π*, n→π* C.T 3A2g(F)→3T1g(P) 3A2g(F)→3T2g(F)	1.75	85	Distorted octahedral
[Cu2(L)Cl2]. H2O	273 357 893	36630 28011 11198	1916 1512 577	Intra-ligand π → π*, n→π* C.T 2Eg→2T2g	1.42	20.6	Distorted octahedral

Thermal Analysis

The thermal decomposition analysis of solid ligand H2L was carried out under argon atmosphere.The weight loss was measured from ambient temperature up to 1000°C.The TGA data clearly indicated that the decomposition of the ligand proceeds in two steps, (Fig 4). The weight loss at the 1st peak, as indicated by the TGA curve at 40-384°C, many attribute to the loss of (C3H6+CO2) segments (obs.=1.7399mg, 18.20%; calc.=1.7389mg, 18.19%). The second step recorded at 384-880°C may indicate the loss of (3H2+NH3+NO2) segment, (obs.=1.1145mg, 14.70%; calc.=1.1016mg,14.60%). The residual weight loss, as indicated by the TGA curve many attributes to the loss of (C23H13N2)

segments, (calc.=5.5112mg,67.19%). the 1st peak may relate to the melting point of the ligand. The thermal decomposition analysis of solid complex [Cr2(L)Cl2] Cl2. h2O was carried out under argon atmosphere. The weight loss was measured from ambient temperature up to 1000°C.The TGA data clearly indicated that the decomposition of the complex proceeds in three steps, (Fig 5). The weight loss at the 1st peak, as indicated by the TGA curve at 46-207°C, many attribute to the loss of (CO+H2O+5H2) segments (obs.= 0.1332mg,7.648%; calc.=0.1327mg,7.622%). The second step recorded at 207-420°C may indicate the loss of (2NH3) segment, (obs.= 0.0818mg, 4.696%; calc.=0.0805mg,4.627%). The third step at 420-805°C is attached to the (C5H10+2Cl2+NH3+NO) segments (obs.=0.6097mg ,35%; calc.=0.6093mg,34.98%). The residual weight loss, as indicated by the TGA curve many attributes to the loss of (2C6H6+C9H5+Cr2O2) segments, (calc.=0.9195mg,52.76%), The thermogram [Mn2(L) (H2O)2] Cl2 complex is proceeds in three steps, (Fig 6). The first peak detected at 100-310°C may be attributed to the loss of a molecule of the (H2O+H2) segments;
(obs.=0.1676mg,2.772%;calc.=0.1672mg,2.766%).The second step recorded at 315-450°C indicated the loss of (NH3+CO+CH4+4H2+H2O) fragments, (obs.=0.772mg, 12.77%;calc.=0.7653mg ,12.66%).The third step recorded at 455-800°C indicated the loss of(CN+CO+Cl2+H2) fragments, (obs.=1.115mg ,18.44%; calc.=1.1090mg, 18.34%). The residual weight loss, as indicated by the TGA curve many attributes to the loss of (C21H8+Mn2O2+2CN) segments, (calc.=4.0045mg,66.23%) and the thermogram [Fe2(L) Cl (H2O)] Cl complex is proceeds in three steps, (Fig 7). The first peak detected at 50-210°C may be attributed to the loss of a molecule of the (H2O+2H2) segments; (obs.=0.0458mg, 3.259%; calc. =0.0446mg, 3.179%). The second step recorded at 210-450°C indicated the loss of (2CO+NH3+H2) fragments, (obs.=0.1570mg,11.18%; calc.=0.1569mg,11.18%). The third step recorded at 450-800°C indicated the loss of (C6H6+3CN+Cl2+C2H8) fragments, (obs.=0.5418mg, 38.56%; calc.= 0.5400mg, 38.43%). the residual weight loss, as indicated by the TGA curve many attributes to the loss of (2C6H6+Fe2O2+C2H4) segments, (calc.=0.6641 mg,47.27%).

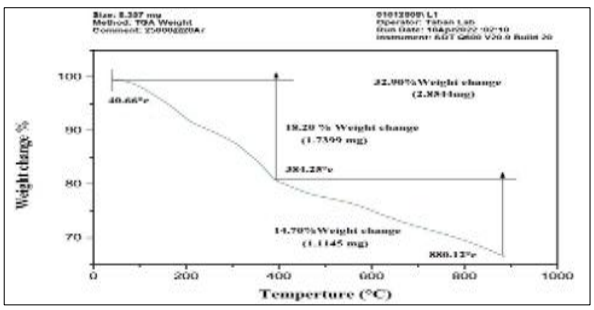

Fig 4: The thermal curves TGA of H_2L in Ar atmosphere.

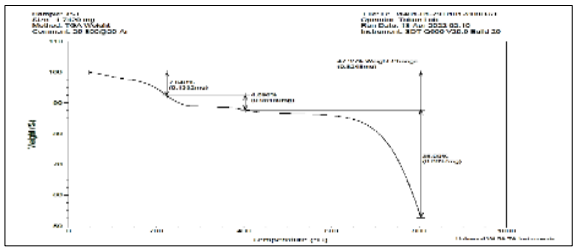

Fig 5: The thermal curves TGA of [Cr_2(L) Cl_2] Cl_2.H_2O in Ar atmosphere.

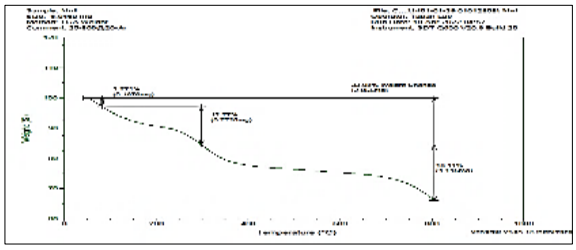

Fig 6: Thermal decomposition of [Mn_2(L) (H_2O)$_2$]in Ar atmosphere.

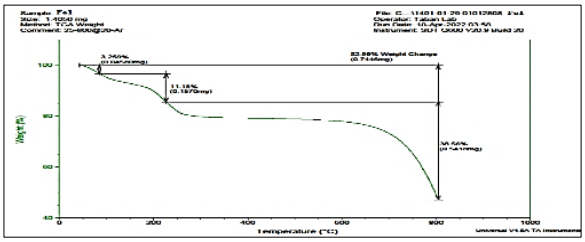

Fig 7: Thermal decomposition of [Fe2(L) Cl (H2O) Cl in Ar atmosphere.

Biological Activity

The antibacterial evaluation of the synthesised ligand H2L and its metal complexes with Cr(Ш), Mn(II), Fe(II), Co(II), Ni(II) and Cu(II)) ions were tested against four types of bacteria: Staphylococcus aureus, Bacillus subtilis, Escherichia coli, and Pseudomonas aeruginosa subtilis Separate investigations carried out using DMSO solutions alone revealed no action against any bacterial strains, confirming the significance of DMSO in biological screening [30-32]. Table (5) shows the results of the tests against the development of several bacterial strains. The impact of the produced ligand and its complexes on the microorganisms under investigation is depicted. The recorded results indicated that complexes were found to be more active; the experimental results concluded the following:

1. All complexes showed activity against positive and negative bacteria.
2. Based on the information gathered, Ni (II) and Cu (II) complexes shows the higher microbiological activity against strains of ((Staphylococcus aureus, Bacillus subtilis) and (Escherichia coli, Pseudomonas auroginosa) bacterial, whereas Cr (III), Mn (II), Fe (II) and Co (II) complexes is less effective against ((Staphylococcus aureus, Bacillus subtilis) and (Escherichia coli, Pseudomonas auroginosa) bacterial.
3. The metal complexes of H2L showed a good exhibit antibacterial activity that is well-matched with Cefotaxime, which would lead to the potential biomedical applications of the

prepared complexes.

The antifungi evaluation of the synthesised ligand H2L and its metal complexes with Cr(Ш), Mn (II), Fe (II), Co (II), Ni (II) and Cu (II)) ions was tested against two types of fungi (Candida albicans and Rhizopus sporium). Separate investigations carried out using DMSO solutions alone revealed no action against fungi organism, confirming the significance of DMSO in biological screening [30-32]. Table (6) shows the results of the tests against the development of two fungi organism. The impact of the produced ligand and its complexes on the microorganisms under investigation is depicted. The recorded results indicated that complexes were found to be more active; the experimental results concluded the following:

1. All complexes showed activity against fungi organism.
2. Based on the information gathered, Fe (II) and Ni (II) complexes showed the higher microbiological activity against two types of fungi (Candida albicans and Rhizopus sporium), whereas Cr (III), Mn (II), Co (II) and Cu (II) complexes are less effective against (Candida albicans and Rhizopus sporium), the tested fungi.
3. The metal complexes of H2L showed a good exhibit, that is well-matched with the Fluconazole, which would lead to the potential biomedical applications of the prepared complexes.

Table (5):The inhibition zones (mm) of anti-bacterial activity for ligand and their complexes.

Compounds	Escherichia coli (G−)	Pseudomonas aeruginosa(G−)	Staphylococcus aureus (G+)	Bacillus stubtilis (G+)
DMSO	-	-	-	-
(Cefotaxime)	17	21	18	15
H_2L	13	17	15	13
$[Cr_2(L)Cl_2].Cl_2H_2O.$	18	27	17	21
$[Mn_2(L)(H_2O)_2].Cl_2.$	23	21	19	19
$[Fe_2(L)(H_2O)Cl]Cl$	17	21	15	22
$[Co_2(L)Cl_2]. .H_2O$	18	19	18	18
$[Ni_2(L)(H_2O)_2]Cl_2$	34	33	32	33
$[Cu_2(L)Cl_2].. H_2O$	25	23	22	24

Table(6): The inhibition zones (mm) of anti-fungal activity for ligand and thier complexes.

Compounds	Candida albicans	Rhizopus sporium
DMSO	--	--
Fluconazole	10	10
H_2L	14	14
$[Cr_2(L)Cl_2].Cl_2H_2O.$	24	25
$[Mn_2(L)(H_2O)_2].Cl_2.$	21	25
$[Fe_2(L)(H_2O)Cl]Cl$	30	34
$[Co_2(L)Cl_2].H2O$	21	22
$[Ni_2(L)(H_2O)_2]Cl_2$	27	26
$[Cu_2(L)Cl_2].. H_2O$	16	16

5. Conclusion

The synthesis of new Schiff-base ligand that are capable to form polymeric complexes and their coordination chemistry with Cr(Ш), Mn (II), Fe (II), Co (II), Ni (II) and Cu (II)) ions are investigated. Schiff-base ligand with the title metal ions resulted in the fabrication of polymeric complexes. The coordination sphere and type of bonding of the complexes were examined using a range of analytical and spectroscopic techniques. These approaches indicated the fabrication of polymeric complexes, in which the geometries around metal centers are six-coordinate complexes were created. The solubility behavior of these complexes and their low magnetic values may account to their polymeric nature. Biological evaluation of ligand and their polymeric complexes against gram-positive bacteria (G+), (Bacillus stubtili, Staphylococcus aureus and gram-negative bacteria (G−), Escherichia coli and Pseudomonas aeruginosa) and compared with antibiotic drug (Cefotaxime) and two types of fungi namely (Candida albicans and Rhizopus sporium) and compared with the activity of fungal agent (Fluconazole).The collected data revealed the antimicrobial activity of the ligand was enhanced upon complex formation.

References

1. Lehn JM (1995) Supramolecular chemistry concepts and perspectives, 1st edn. Wiley-VCH, Weinheim.
2. Belghoul B, Welterlich W, Maier A, Toutianoush A, Rabindranath AR, Tieke B (2007) Langmuir 23:5062. doi:10.1021/la062044c.
3. El-Bindary AA (1998) Synth React Inorg Met Org Chem 28:1743.
4. Kannan RM, Kolhe P, Misra E, Kannan S, Lieh-Lai M (2003) Int J Pharm 259:143. doi:10.1016/S0378-5173(03)00225-4.
5. Si SF, Tang JK, Liao DZ, Jiang ZH, Yan SP (2002) Inorg Chem Commun 5:76. doi:10.1016/S1387-7003(01)00349-5.
6. El-Sonbati AZ, El-Bindary AA, Diab MA (2003) Spectrochimica Acta Part A 59:443. doi:10.1016/S1386-1425(02)00222-6.
7. Biswas M, Moitra S (1989) J Appl Polym Sci 38:1243. doi: 10.1002/app.1989.070380705
8. Camarillo R, Canzares P, Perez A (2002) Desalination 144:279.

doi:10.1016/S0011-9164(02)00328-4.
9.Reddy AR, Reddy KH (2003) Proc Indian Acad Sci (Chem Sci) 115:155. doi:10.1007/BF02704254.
10. Sahiner N, Pekel N, Guven O (1998) Radial Phys Chem 52:271. doi:10.1016/S0969-806X(98)00195-9.
11.MJ Al-Jeboori, AH Al-Dujaili, AE Al-Janabi (2009) Coordination of carbonyl oxygen in the complexes of polymeric Ncrotonyl-2-hydroxyphenylazomethine, Transition Met. Chem., 34: 109-113.
12. Andruh M (2005) Pure Appl Chem 77:1685. doi:10.1351/pac 200577101685
13. Elermany Y, Kara H, Elmali A (2003) Z Naturforsch 58a:363.
14 Al-Jeboori M.J., Hasan Ahmad Hasan and Worood A. Jaafer Al-Sa'idy, Formation of polymeric chain assemblies of transition metal complexes with a multidentate Schiff-base). Transition Met Chem, 34, 593–598, (2009).
15.G. I. Koldobskii, V. A. Ostrovskii, B. V. Gidaspov, Chem. Heterocycl. Compd., 16, 665–674 (1980).
16.Parikh, V. M. Absorption spectroscopy of organic molecules. Reading, Mass.: Addison-Wesley Publishing Company,1974.
17. Nair, M. S., Arish, D., & Johnson, J. Synthesis, characterization and biological studies on some metal complexes with Schiff base ligand containing pyrazolone moiety. Journal of Saudi Chemical Society,2016, 20, S591-S598.
18 SilverschtienR.M., Bassler and Morril, "Spectrophotometers Indentification of Organic Compound", Translated by Ali Hussain and Suphi Al-Azawi. 1981.
19. Issa O. Issa, Mohamad J. Al-Jeboori* and Jassim S. Al-Dulaimi, "Formation of binuclear metal complexes with multidentate Schiff-base oxime ligand: synthesis and spectral investigation", Journal of Ibn Al-Haitham for Pure and Applied Sciences, Vol. 22, No. 2, 142-153, (2011).
[20] Hasan A. H, Enaam I.Y and Ahmed K. H. Journal of Plant Archives,2020, 20 (1). pp. 2405-2411.
21 Faliah Hassan Ali Al-Jeboori, Mohamad Jaber Al-Jeboori and Abdul Muhsin Al-Haidari, "Synthesis and structural characterization of some transition metal complexes with cyclic N2OS2 ligand", J. Chem. Pharm. Res., 5(8), 203-216, (2013).
22. F. H. A. Al-Jeboori, K. K. Hammud, M. J. Al-Jeboori," Synthesis and characterization of new acyclic octadentate ligand and its complexes" Iranian Journal for Science & Technology, 38A (4): 489-497, (2014).
23.A. L. Pochodylo, R. L. LaDuca, Inorg. Chem. Comm., 14, 722-726 (2011).
24. M. Tumer, C. Celik, H. Koksal, S. Serin. Transition Met. Chem., 24, 525 (1999)
25.Safaudeen A. Hussain and Mohamad J. Al-Jeboori, "New Metal Complexes Derived from Mannich-Base Ligand; Synthesis, Spectral Characterisation and Biological Activity", Journal of Global Pharma Technology, 11(2), 548-560, (2019).
26.Sharghi, H., & Jokar, M. Highly stereoselective facile synthesis of β-amino carbonyl compounds via a Mannich-type reaction catalyzed by γ-Al2O3/MeSO3H (alumina/methanesulfonic acid: AMA) as a recyclable, efficient, and versatile heterogeneous catalyst. Canadian Journal of Chemistry,2010, 88(1), 14-26.
27. Ramachandran, E., Gandin, V., Bertani, R., Sgarbossa, P., Natarajan, K., Bhuvanesh, N. S., & Marzano, C. Synthesis, characterization and cytotoxic activity of novel copper (II) complexes with aroylhydrazone derivatives of 2-Oxo-1, 2-dihydrobenzo[h] quinoline-3-carbaldehyde. Journal of Inorganic Biochemistry, 2018,182, 18-28.
28. Ho J, Lee WY, Koh KJT, Lee PPF, Yan YK. Rhenium(I) tricarbonyl complexes of salicylaldehyde semicarbazones: Synthesis, crystal structures and cytotoxicity, Journal of Inorganic Biochemistry,2013, 119: 10-20.
29.Lever, A. P. Inorganic electronic spectroscopy. Studies in physical and theoretical chemistry,1984, 33.
30.Al-Jeboori M. J., Hasan H. A. and Yousif E. I., (2012). "Metal-assisted assembly of dinuclear metal(II) dithiocarbamate Schiff-base macrocyclic complexes: Synthesis and biological studies", Global J. Inorg. Chem, 3. 10. 1-7.
31.. Enaam Ismail Yousif, Nihad Kadhum Hasan and Mohamad J. Al-Jeboori* (New Metal Complexes of Thiosemicarbazone Mannich base Ligand; Synthesis, Structural Characterisation and Biological Activity P J M H S Vol. 16, No. 06, Jun 2022 565.
32.Enaam I. Y (2018) Journal of Global Pharma Technology. 10(03):875-882.